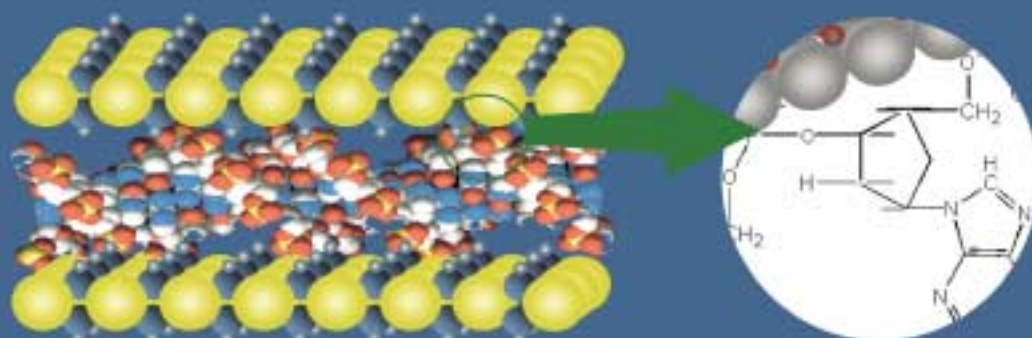
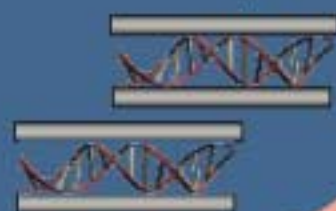


# Soluble Inorganic Vector

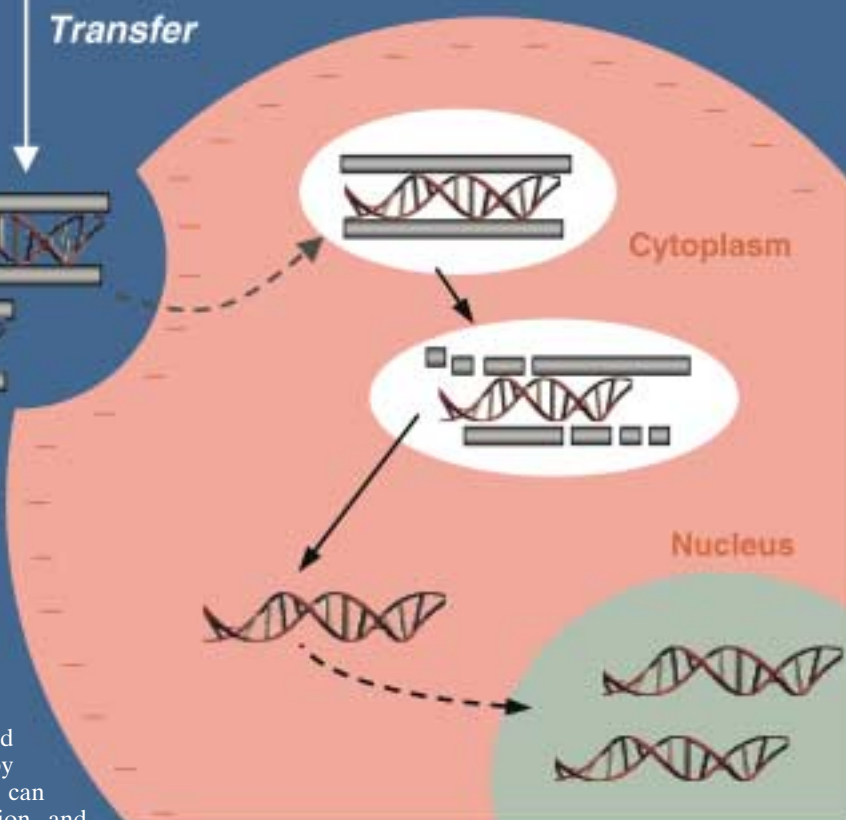


DNA-LDH nanohybrid

*Transfer*



**Recognition  
and uptake  
(Endocytosis)**



Negatively charged biomolecules—DNA fragments, for example—can be stably intercalated into a layered double hydroxide (LDH), the anionic clay formed from cationic brucite-like layers, by simple ion exchange. The LDH can protect the DNA from degradation, and the charge neutralization enhances the transfer of the DNA-LDH hybrid into mammalian cells through endocytotic means. Once within the cells however, the slightly acidic lysosome dissolves the LDH and thereby exposes the intercalated molecule: The biomolecular-inorganic hybrid can deliver drugs or genes from the noncytotoxic carrier. Find out more on the following pages.

# Inorganic Layered Double Hydroxides as Nonviral Vectors\*\*

Jin-Ho Choy,\* Seo-Young Kwak, Yong-Joo Jeong, and Jong-Sang Park

Layered double hydroxides (LDHs), the so-called anionic clays, consist of cationic brucite-like layers and exchangeable interlayer anions (Figure 1 A).<sup>[1]</sup> The unique anion exchange capability of LDHs meets the requirement of inorganic matrices for encapsulating functional biomolecules with negative charge in aqueous media (Figure 1 B). Such biomolecules can be incorporated between hydroxide layers by a simple ion-exchange reaction to form bio-LDH nanohybrids.<sup>[2]</sup> The negatively charged biomolecules intercalated in the gallery spaces would gain extra stabilization energy due to the electrostatic interaction between cationic brucite layers and anionic biomolecules, as depicted in Figure 1 C. Here, the hydroxide layers can play the role of a reservoir to protect intercalated DNA from DNase degradation. However, if desired, the hydroxide layers can be intentionally removed by

dissolving in an acidic media, which offers a way of recovering the encapsulated biomolecules. We have also found that the hybridization between cationic layers and anionic biomolecules would greatly enhance the transfer efficiency of biomolecules into mammalian cells or organs, as illustrated in Figure 1 D. The charge neutralization through hybridization of hybrids into cells through endocytosis,<sup>[3]</sup> since it greatly reduces the electrostatic repulsive interaction between negatively charged cell membranes and anionic biomolecules during this process. Once bio-LDH hybrids are introduced into cells, the hydroxide layer in the bio-LDH hybrids would then be removed slowly in the lysosome, where the pH is slightly acidic (pH 4–5), because the hydroxide layers of Mg and Al dissolve in an acidic environment. At the same time, interlayer biomolecules would be partially replaced by other anions in the cell electrolyte in such a way that the encapsulated biomolecules could be released in the inside of a cell from an LDH hybrid. In this report, our primary attention was focused on verifying the possible applications of bio-LDH hybrids as gene or drug delivery carriers by a systematic experimental approach.

The first step is to prepare a two-dimensional LDH compound with an appropriate ion-exchange capacity and bio-compatibility. LDHs can be simply prepared by coprecipitation of mixed metal ions ( $\text{Mg}^{2+}/\text{Al}^{3+} = 2/1$ ) with base (0.1N NaOH, pH  $\approx 10$ ) from aqueous solutions under nitrogen. The resulting white precipitate was washed with decarbonated water for several times, freeze-dried for chemical analysis,<sup>[4]</sup> and then treated with each biomolecule. The pristine  $\text{Mg}_{0.68}\text{Al}_{0.32}(\text{OH})_2 \cdot (\text{NO}_3^-)_{0.32} \cdot 1.2\text{H}_2\text{O}$  ( $\text{Mg}_2\text{Al-NO}_3^-$ -LDH) has a well developed layer structure with the basal spacing of 8.7 Å (Figure 2 a), which corresponds to the sum of the gallery height of 3.9 Å (the thickness of ionic  $\text{NO}_3^-$ ) and the thickness of brucite-like layer itself (4.8 Å). The second step is to replace interlayer nitrate ions in LDH with biomolecules or others. Upon replacement with herring testis DNA, adenosine triphosphate (ATP), fluoresceine 5-isothiocyanate (FITC), or *c-myc* antisense oligonucleotide (*As-myc*) by simple ion-exchange reaction,<sup>[5]</sup> the basal spacings are expanded further to 23.9, 19.4, 18.8, and 17.1 Å,

respectively (Figure 2 b–e), to indicate that the biomolecules have been successfully intercalated into the hydroxide layers to form bio-LDH hybrids. The observed gallery height of 19.1 Å ( $= 23.9 - 4.8$  Å) in the DNA-LDH hybrid is consistent with the thickness of a DNA molecule ( $\approx 20$  Å)<sup>[6]</sup> in a double helical conformation lying parallel to the basal plane of hydroxide layers. The slight discrepancy between observed and expected gallery height is surely due to the spatial confinement of DNA molecules through strong electrostatic interactions between the DNA phosphate groups and the positively charged hydroxide layers (Figure 1 C, inset).<sup>[2]</sup> The

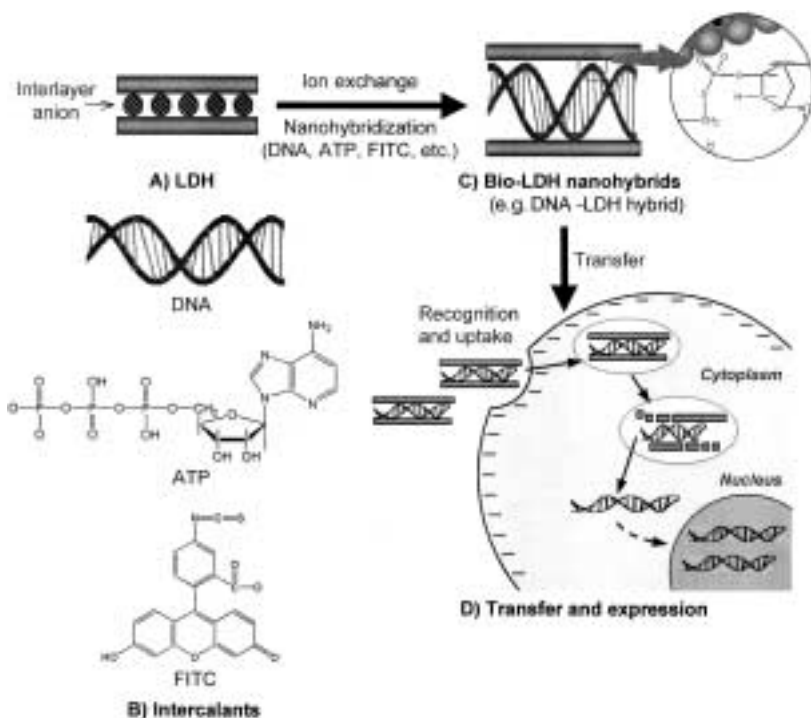


Figure 1. Schematic illustration of the hybridization and expected transfer mechanism of the bio-LDH hybrid into a cell.

[\*] Prof. Dr. J.-H. Choy, Dipl.-Chem. S.-Y. Kwak, Dr. Y.-J. Jeong, Prof. J.-S. Park  
National Nanohybrid Materials Laboratory (NNML)  
School of Chemistry and Molecular Engineering  
Seoul National University, Seoul 151-747 (Korea)  
Fax: (+82)2-872-9864  
E-mail: jhchoy@plaza.snu.ac.kr

[\*\*] This work was in part supported by the Korean Ministry of Science and Technology through the NRL project and by the Korean Ministry of Education (BSRI-99-3413). S.Y.K. expresses her thanks to the BK21 fellowship.

Supporting Information for this article is available on the WWW under <http://www.wiley-vch.de/home/angewandte/> or from the author.

interlayer separations for the ATP-LDH and FITC-LDH hybrids (14.6 and 14.0 Å) are also in good agreement with the respective molecular dimensions of the guest species,<sup>[7]</sup> assuming that they are oriented toward the hydroxide plane to maximize the electrostatic attractions.

We also performed cellular uptake experiments using FITC as a probe to verify the delivery potential. As shown in

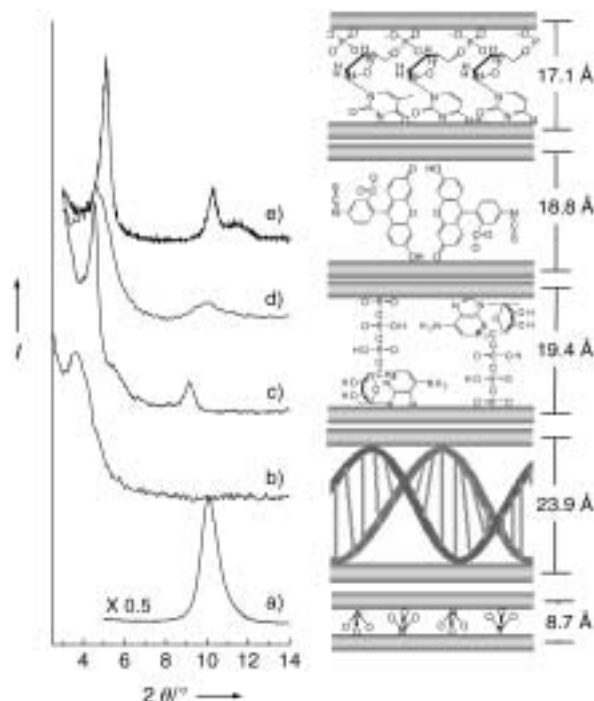


Figure 2. Powder X-ray diffraction patterns for a) pristine  $\text{Mg}_2\text{Al}(\text{NO}_3)_2$ -LDH, b) DNA-LDH, c) ATP-LDH, d) FITC-LDH, and e) As-myc-LDH. The XRD patterns were obtained with a powder diffractometer (PW3710, Philips) equipped with Ni-filtered  $\text{CuK}\alpha$  radiation ( $\lambda = 1.5418$  Å). The separation of the layers upon intercalation is shown schematically on the right.

Figure 3A, the uptake of cellular hybrid becomes more significant with increasing concentration. At the same time, the longer that the cellular incubation time is, the higher the cellular uptake rate becomes (Figure 3B). This implies that the hybrids can enter into cells effectively in both time- and dose-dependent manners. Further evidence on cellular uptake of the FITC-LDH hybrid was obtained directly from laser scanning confocal microscopy experiments.<sup>[8]</sup> Solutions of FITC-LDH hybrids (1 and 3  $\mu\text{M}$ ) were added to NIH3T3 cells and then incubated for 1, 4, or 8 h. The cells were then washed with phosphate buffer solution (PBS) and fixed with formaldehyde (3.7%) prior to measurement. Figure 4 shows the cellular localization of the fluorophore obtained after a fixed incubation time. The fluorophores are detected in cells within an hour of incubation, and the fluorescence intensities continuously increase over 8 h. The fluorophores in the cells are distributed primarily in the peripheral and cytosol regions, with some in the nucleus. Moreover, as expected from Figure 3, the cells treated with 3  $\mu\text{M}$  of FITC-LDH show more intense fluorescence than those treated with 1  $\mu\text{M}$  (Figure 4). In contrast, the cells treated with 5  $\mu\text{M}$  FITC remain dark regardless of incubation time because cells could not take up FITC itself even at high concentration. It is

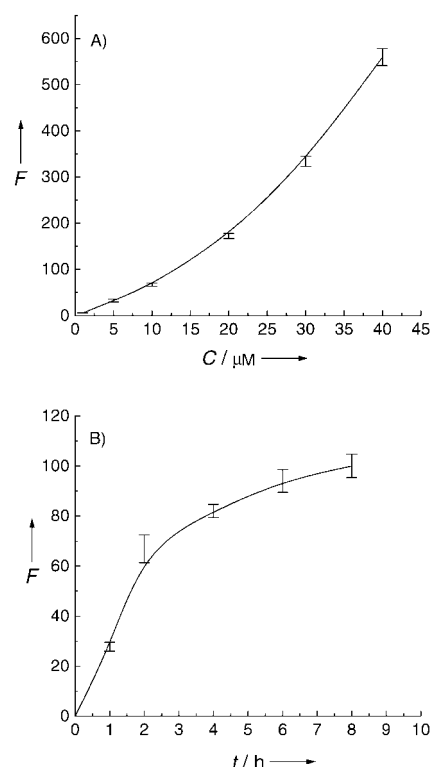


Figure 3. Cellular uptake kinetic profiles of FITC-LDH into cells at A) various concentrations of the FITC-LDH hybrid and at B) different incubation times.

obvious that LDH plays an important role in mediating the cellular uptake of FITC. All the cells can engulf the neutralized nanoparticles through phagocytosis or endocytosis. Further, FITC in the hybrid can be partially released by ion-exchange reactions, at physiological salt conditions, over 8 h and that LDHs, as encapsulating materials, dissolve gradually in a weak acidic solution. Therefore, we conclude that the intracellular fluorescence has been created by deintercalated FITC and some by FITC-LDH hybrids in the cell.

We are also able to demonstrate that antisense oligonucleotides enter into cells and participate in the process of cell division. The As-myc were intercalated into LDH and transferred into cells. LDHs themselves have no discernible cytotoxic effect on HL-60 cells, the human promyelocytic leukemia cell line, when administered at levels below 1000  $\mu\text{g mL}^{-1}$  for up to 4 days. The effect of As-myc-LDH hybrid on the growth of HL-60 cells is shown in Figure 5. The

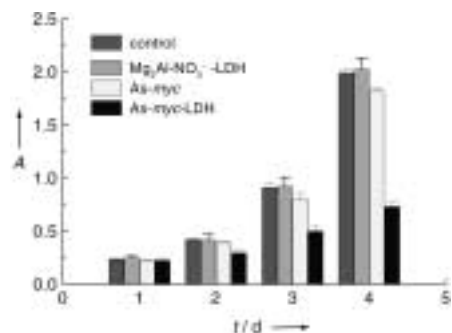


Figure 5. Effect of As-myc and the As-myc-LDH hybrids on the growth of HL-60. Each material was present at 20  $\mu\text{M}$ .

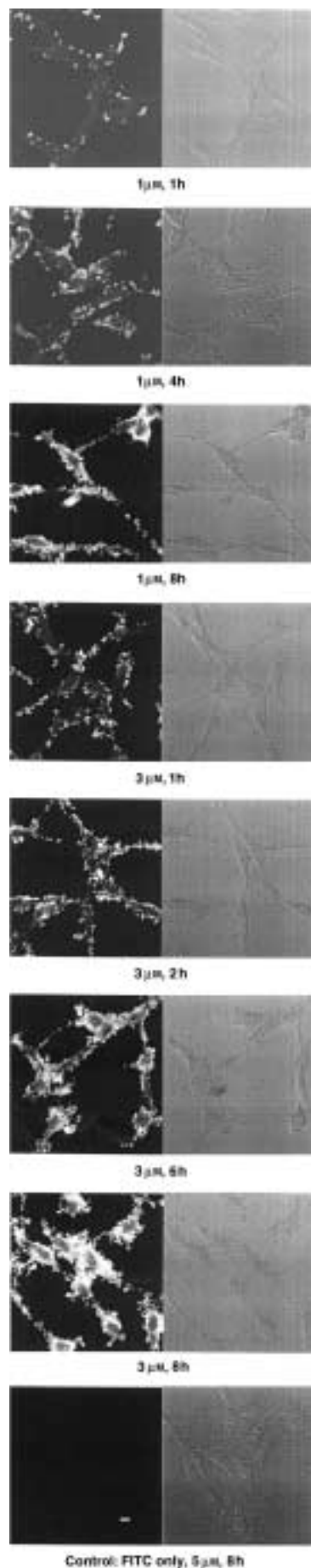


Figure 4. Laser confocal fluorescence microscopic images (left) and phase contrast micrographic images (right) of NIH3T3 cells. The scale bar is 10  $\mu\text{m}$ .

cells have been exposed to As-myc-LDH hybrids at a concentration of 20  $\mu\text{M}$  and incubated for 4 days (see Experimental Section and ref. [9]). During incubation, cell viability was measured daily by a MTT assay (a colorimetric assay that measures the reduction of 3-(4,5-dimethylthiazol-2-yl)-2,5-diphenyl tetrazolium bromide (MTT reagent) by mitochondrial succinate dehydrogenase) and compared to a control free of As-myc. According to Figure 5, HL-60 cells in a culture treated with the As-myc-LDH hybrid exhibit time-dependent inhibition of proliferation, which indicates 65 % growth inhibition compared to the untreated cells. These results imply that As-mycs are internalized in the cells and eventually inhibit the growth of cancer cells. However, no significant inhibition effect is observed for the cells treated only with As-myc, as expected.

In conclusion, we demonstrated that inorganic supramolecules, such as the nanoscale LDHs, can act as biomolecule reservoirs and gene and drugs carriers. Cellular uptake experiments reveal that the FITC-LDH hybrid is effectively transferred into NIH3T3 cells and, when the HL-60 cells are incubated with the As-myc-LDH hybrid, a strong suppression of cancer cell growth (65 %) is observed. LDH itself is noncytotoxic towards HL-60, a type of leukemia cell. Therefore, LDHs can act as new inorganic carriers, completely different from existing nonviral vectors in terms of its chemical nature.

#### Experimental Section

**Samples:** Prior to the DNA exchange, the herring testis DNA (D-6898, Sigma) was dissolved in water (10  $\text{mg mL}^{-1}$ ). The solution was extracted by phenol and then by a phenol/chloroform (1/1) mixture. The recovered aqueous phase was passed rapidly through a 17-gauge hypodermic needle 15 times to shear DNA molecules to 500–1000 base pairs (bp). The sheared DNA was precipitated by adding ice-cold ethanol, followed by centrifugation to collect the purified DNA molecules, which were subsequently redissolved in deionized water (10  $\text{mg mL}^{-1}$ ).  $\text{Mg}_2\text{Al-NO}_3$ -LDH was prepared by the aqueous coprecipitation of  $\text{Mg}^{2+}$  and  $\text{Al}^{3+}$  (0.024 and 0.012 M) with base (0.1 N NaOH) under nitrogen. During titration, the solution pH and temperature were adjusted to  $10 \pm 0.2$  and  $60^\circ\text{C}$ . The resulting white precipitate was aged for 24 h, collected by centrifugation, then washed thoroughly with decarbonated water. Biomolecules (herring testis DNA, ATP, FITC) were intercalated into  $\text{Mg}_2\text{Al-NO}_3$ -LDH at pH 7 for 48 h at  $60^\circ\text{C}$ .

**Cellular uptake kinetic profiles:** Various amounts of FITC-LDH were added to  $8 \times 10^4$  NIH3T3 cells and incubated for 2 h. The FITC-LDH hybrid (10 mM) was added to the cells and incubated for 1, 2, 4, 6, or 8 h. After incubation, the samples were washed with PBS buffer, lysed with 1 % Triton X-100 in PBS, then incubated further at room temperature for 15 minutes. The samples were collected by scraping all areas of the plate surface. The detached cells were centrifuged to remove cell debris and to collect supernatant. The relative fluorescence intensity of the collected supernatant was measured ( $\lambda_{\text{ex}} = 494$ ,  $\lambda_{\text{em}} = 520$  nm) against a FITC-only control experiment.

**Microscopy:** NIH3T3 cells were grown on round coverslips in a 12-well culture plate and cultured for a day. FITC-LDH hybrids (1 and 3 mM) were added to the cells ( $6 \times 10^4$  per coverslip) and incubated for 1, 2, 4, 6, or 8 h. For comparison, control experiments were performed with only FITC (5 mM) itself under the same conditions. All of the samples were washed three times with the PBS buffer and fixed with formaldehyde in PBS (3.7 %). After washing again with PBS, the samples were observed with a laser scanning confocal microscope (LSM 410, Zeiss). The samples were excited by an argon laser ( $\lambda = 488$  nm) and the images subject to a longpass filter (515 nm).<sup>[8]</sup>

Cytotoxicity: HL-60 (human promyelocytic leukemia) cells were cultured in a 24-well culture plate ( $5 \times 10^4 \text{ mL}^{-1}$ ). The cells were exposed to various amounts of LDH ( $1-1000 \mu\text{g mL}^{-1}$ ). A control experiment was performed without LDH under the same conditions. Cell viability was determined daily over four days by an MTT assay.<sup>[9]</sup>

HL-60 cell growth: HL-60 cells were cultured in a 24-well culture plate ( $5 \times 10^4 \text{ mL}^{-1}$ ). The cells were exposed to As-myc-LDH ( $20 \mu\text{M}$ ). The sequence of As-myc is 5'-d-(AACGTTGAGGGGCAT)-3' and complementary to the initiation codon and the next four codons of c-myc mRNA. Control experiments were performed with only As-myc ( $20 \mu\text{M}$ ) and without As-myc or As-myc-LDH complex under the same conditions. Cell viability was determined daily over four days by MTT assay.<sup>[9]</sup>

Received: March 24, 2000

Revised: May 30, 2000 [Z14893]

- [1] F. Cavani, F. Trifiro, A. Vaccari, *Catal. Today* **1991**, *11*, 173–301.
- [2] J. H. Choy, S. Y. Kwak, J. S. Park, Y. J. Jeong, J. Portier, *J. Am. Chem. Soc.* **1999**, *121*, 1399–1400.
- [3] a) F. D. Ledley, *Hum. Gene Therapy* **1995**, *6*, 1129–1144; b) S. S. Davis, *Trends Biotechnol.* **1997**, *15*, 217–224.
- [4] The chemical formula for the pristine  $\text{Mg}_{0.68}\text{Al}_{0.32}(\text{OH})_2(\text{NO}_3^-)_{0.32} \cdot 1.2\text{H}_2\text{O}$ , was determined by inductively coupled plasma and elemental analyses.
- [5] a) V. R. L. Constantino, T. J. Pinnavaia, *Inorg. Chem.* **1995**, *34*, 883–892; b) M. Meyn, K. Beneke, G. Lagaly, *Inorg. Chem.* **1993**, *32*, 1209–1215.
- [6] a) R. R. Sinden, *DNA Structure and Function*, Academic Press, New York, **1994**; b) J. O. Rädler, I. Koltover, T. Saldit, C. R. Safinya, *Science* **1997**, *275*, 810–814.
- [7] L. Streyer, *Biochemistry*, 4th ed., W. H. Freeman, New York, **1995**.
- [8] a) R. J. Lee, P. S. Low, *J. Biol. Chem.* **1997**, *269*, 3198–3204; b) Z. W. Lee, S. M. Kwon, B. C. Kim, S. H. Leem, I. Shin, J. H. Kim, K. S. Ha, *J. Biol. Chem.* **1998**, *273*, 12710–12715; c) K. Vogel, S. Wang, R. J. Lee, J. Chmielewski, P. S. Low, *J. Am. Chem. Soc.* **1996**, *118*, 1581–1586.
- [9] a) E. L. Wickstrom, T. A. Bacon, A. Gonzalez, D. L. Freeman, G. H. Lyman, E. Wickstrom, *Proc. Natl. Acad. Sci. USA* **1998**, *85*, 1028–1032; b) M. B. Hansen, S. E. Nielsen, K. Berg, *J. Immunol. Methods* **1989**, *119*, 201–203.

## Epoxidation Catalysis by a Manganese Corrole and Isolation of an Oxomanganese(v) Corrole\*\*

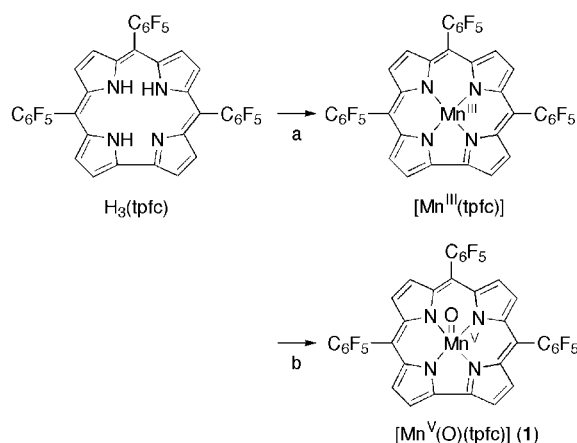
Zeev Gross,\* Galina Golubkov, and Liliya Simkhovich

The milestones in metalloporphyrin-catalyzed oxygenation of hydrocarbons are the 1979 and 1980 publications of Groves, Hill, and their coworkers about the utilization of iron(III) and manganese(III) porphyrins as catalysts for the epoxidation of olefins by iodosylbenzene.<sup>[1]</sup> Similar mechanisms were proposed in both cases, oxygen atom transfer from iodosylbenzene to the catalyst to form a *formally* oxometal(v) porphyrin

intermediate, which subsequently transfers its oxygen atom to the substrate.<sup>[2]</sup> But, while trapping and extensive spectroscopic characterization of the intermediate in the iron porphyrin catalysis started as soon as 1981,<sup>[3]</sup> oxomanganese(v) porphyrins remained elusive for a very long time.<sup>[4]</sup> Only in 1999 did Jin and Groves succeed in obtaining the  $^1\text{H}$  NMR spectrum of such a complex, the diamagnetism of which provides the strongest proof of the structure.<sup>[5]</sup>

Recently we got involved in the chemistry of corroles; long known tetrapyrroles, whose skeleton may be viewed as either the one carbon atom short analogues of porphyrins or as the aromatic version of corrin, the ligand bound to cobalt in the coenzyme of Vitamin B<sub>12</sub>.<sup>[6, 7]</sup> We first introduced an extremely facile synthesis of 5,10,15-tris(pentafluorophenyl)corrole ( $\text{H}_3(\text{tpfc})$ ),<sup>[8, 9]</sup> from which a novel class of chiral macrocycles can easily be obtained.<sup>[10]</sup> In addition, we have demonstrated that the metal complexes of  $\text{H}_3(\text{tpfc})$  are potent catalysts.<sup>[11]</sup> Specifically, the iron(IV) complex  $[\text{Fe}(\text{tpfc})\text{Cl}]$ -catalyzed the oxygen-atom transfer from iodosylbenzene to both styrene and ethylbenzene. Assuming an analogy to metalloporphyrin catalysis, in which manganese complexes are equally or even more active than iron porphyrins,<sup>[2a]</sup> we decided to investigate manganese corroles.<sup>[12]</sup> Motivation for the present research was that the ability of corroles to stabilize high oxidation states is superior to that of porphyrins,<sup>[13]</sup> the thermal stability of iron(IV) corroles being the most relevant example.<sup>[14]</sup> Herein we report that the manganese(III) complex  $[\text{Mn}(\text{tpfc})]$  is an interesting epoxidation catalyst and the successful isolation of an oxomanganese(v) corrole.

The metallation of  $\text{H}_3(\text{tpfc})$  was achieved in high yields by reaction with excess  $\text{Mn}(\text{OAc})_2 \cdot 4\text{H}_2\text{O}$  in DMF (Scheme 1).<sup>[15]</sup>



Scheme 1. Synthesis of  $[\text{Mn}^{\text{III}}(\text{tpfc})]$  and  $[\text{Mn}^{\text{V}}(\text{O})(\text{tpfc})]$  (1) a)  $\text{Mn}(\text{OAc})_2 \cdot 4\text{H}_2\text{O}$ , DMF, reflux; b)  $\text{CH}_2\text{Cl}_2$ ,  $\text{O}_3$ ,  $-78^\circ\text{C}$ .

[\*] Prof. Dr. Z. Gross, G. Golubkov, L. Simkhovich  
Department of Chemistry and  
Institute of Catalysis Science and Technology  
Technion – Israel Institute of Technology  
Haifa 32000 (Israel)  
Fax: (+972)-4-8233735  
E-mail: chr10zg@tx.technion.ac.il

[\*\*] We acknowledge the partial support of this research by “The Fund for the Promotion of Research at the Technion”.

Identification of the reaction product as  $[\text{Mn}^{\text{III}}(\text{tpfc})]$  (corroles are trianionic ligands) is based on a combination of mass spectroscopy, NMR, and UV/Vis spectroscopy, and comparison to reported manganese corroles. Interestingly, both the green color and the UV/Vis spectrum of  $[\text{Mn}(\text{tpfc})]$  (Figure 1a) are remarkably similar to that of manganese(III) porphyrins.<sup>[16]</sup> Most relevant are the split Soret band and the